Chemistry of NO$_x$ on TiO$_2$ Surfaces Studied by Ambient Pressure XPS: Products, Effect of UV Irradiation, Water, and Coadsorbed K$^+$

Olivier Rosseler,[†,‡] Mohamad Sleiman,[†] V. Nahuel Montesinos,[§,∥,⊥] Andrey Shavorskiy,[†] Valerie Keller,[‡] Nicolas Keller,[‡] Marta I. Litter,[§,∥] Hendrik Bluhm,[†] Miquel Salmeron,[†,#] and Hugo Destaillats*[,†]

[†]Lawrence Berkeley National Laboratory, Environmental Energy Technologies Division, Material Sciences Division, Chemical Sciences Division and Advanced Light Source, Berkeley, California, United States

[‡]Université de Strasbourg, Institut de Chimie et Procédés pour l'Energie, l'Environnement et la Santé (ICPEES), CNRS, Strasbourg, France

[§]Comisión Nacional de Energía Atómica, Gerencia Química, San Martín, Pcia. de Buenos Aires, Argentina

[∥]Consejo Nacional de Investigaciones Científicas y Técnicas, Buenos Aires, Argentina

[⊥]INQUIMAE, DQIAQyF, Facultad de Ciencias Exactas y Naturales, Universidad de Buenos Aires, Argentina

[#]Materials Science Division, Lawrence Berkeley National Laboratory and Materials Science and Engineering Department, University of California, Berkeley, California, United States

S *Supporting Information*

ABSTRACT: Self-cleaning surfaces containing TiO$_2$ nanoparticles have been postulated to efficiently remove NO$_x$ from the atmosphere. However, UV irradiation of NO$_x$ adsorbed on TiO$_2$ also was shown to form harmful gas-phase byproducts such as HONO and N$_2$O that may limit their depolluting potential. Ambient pressure XPS was used to study surface and gas-phase species formed during adsorption of NO$_2$ on TiO$_2$ and subsequent UV irradiation at λ = 365 nm. It is shown here that NO$_3^-$, adsorbed on TiO$_2$ as a byproduct of NO$_2$ disproportionation, was quantitatively converted to surface NO$_2$ and other reduced nitrogenated species under UV irradiation in the absence of moisture. When water vapor was present, a faster NO$_3^-$ conversion occurred, leading to a net loss of surface-bound nitrogenated species. Strongly adsorbed NO$_3^-$ in the vicinity of coadsorbed K$^+$ cations was stable under UV light, leading to an efficient capture of nitrogenated compounds.
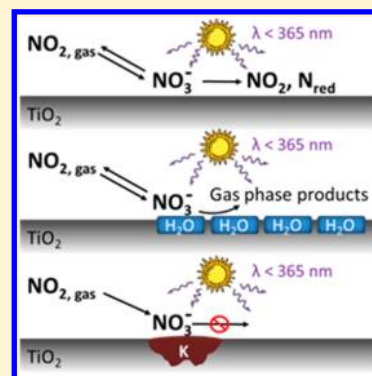
SECTION: Environmental and Atmospheric Chemistry, Aerosol Processes, Geochemistry, and Astrochemistry

Raising nitrogen oxide (NO$_x$) levels are a concern for air quality in metropolitan areas. Large-scale deployment of urban surfaces functionalized with photoactive TiO$_2$ has been postulated to be an effective approach for improving urban air through the abatement of NO$_2$, a toxic pollutant and ozone precursor.[1] Photocatalytic *denoxification* proceeds by oxidizing adsorbed nitrogen oxides to nitrate anions (NO$_3^-$), thus irreversibly removing NO$_x$ from the atmosphere.[2] However, other reactions may take place that involve the formation of other nitrogenated species such as NO, N$_2$O, and HONO, which can be released back to the gas phase and lead to partial *renoxification*. Similarly, TiO$_2$ is a minor component of mineral dust particles and has recently been shown to be partially responsible for the photochemical reactivity of atmospheric mineral aerosols. Reactions between NO$_2$ and mineral dust account for some of the photochemical sources of daytime HONO.[3−6]

To better understand the interaction of NO$_2$ with TiO$_2$ and the role of UV light, humidity, and cationic impurities, we used ambient pressure X-ray photoelectron spectroscopy (APXPS)[7] under 0.05 Torr of NO$_2$ (equivalent to 70 ppmv) to monitor the different oxidation states of nitrogen species, adsorbed on TiO$_2$ or in the gas phase, and their evolution with time under UV irradiation. We observed a UV-induced overall reduction of the nitrogenated species, leading to their partial depletion from the TiO$_2$ surface. These reactions seem to be favored by the introduction of water vapor and hindered by the presence of potassium cations on the surface of the TiO$_2$ single crystal.

Surface Spectra. We monitored the reactions of NO$_2$ adsorbed on anatase (101). Figure 1a illustrates surface N1s APXPS spectra obtained before and after 0.05 Torr of NO$_2$ was admitted into the chamber and allowed to equilibrate with the surface in the dark and after 160 min of UV irradiation. The corresponding Ti2p, O1s, and C1s spectra are presented in Figure 1b−d, respectively. A description of the peak fitting methodology is provided in the Supporting Information. The Ti2p spectra (Figure 1b) shows a fully oxidized TiO$_2$ due to healing of Ti^{3+} defects observed upon the introduction of NO$_2$
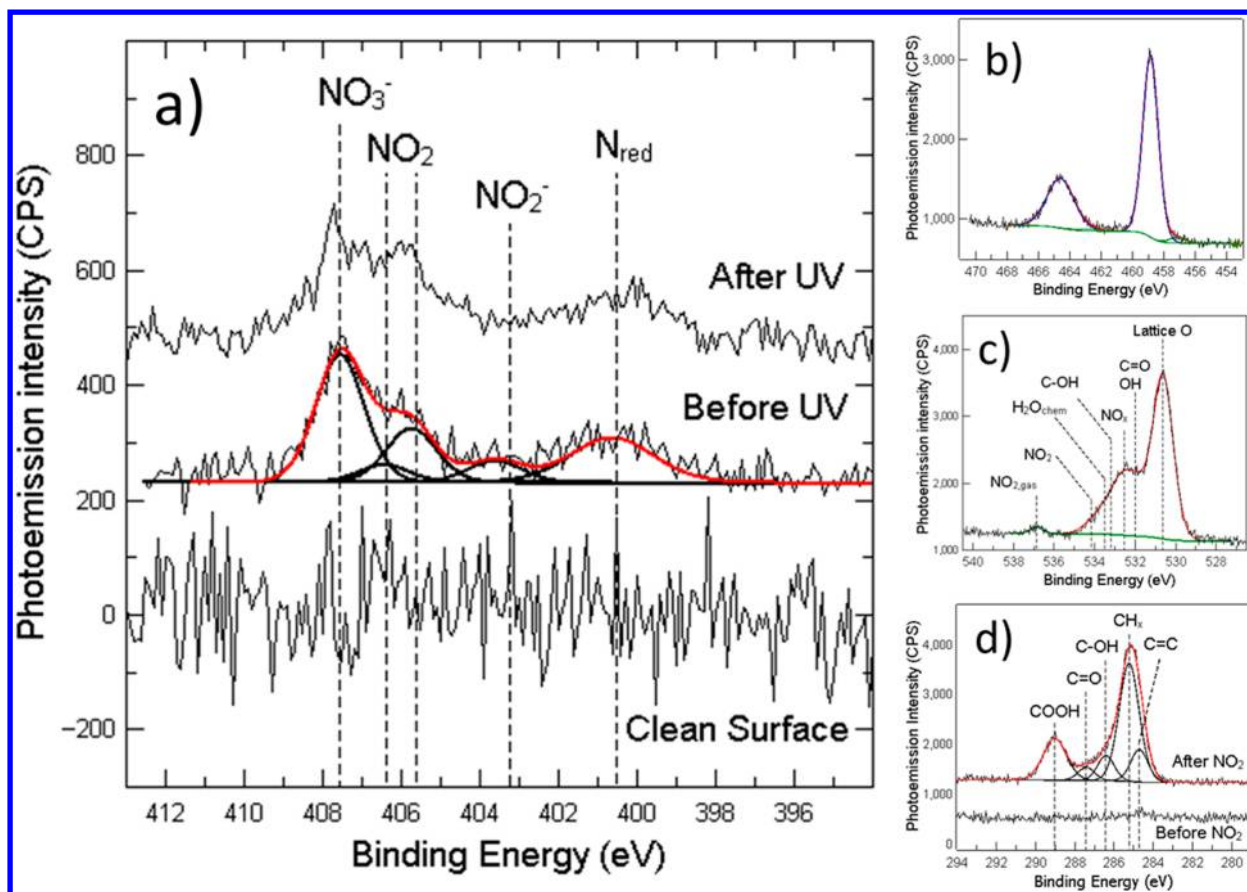
Figure 1. APXPS spectra on TiO_2 surface in the dark at 293 K for (a) N1s on the clean surface and the surface exposed to 0.05 Torr NO_2 before and after UV irradiation (linear background subtracted); (b) Ti2p after introducing NO_2; (c) O1s after introducing NO_2; and (d) C1s on the clean surface and exposed to 0.05 Torr NO_2.

(10^{-6} Torr and up, Figure S2 in the Supporting Information). The O1s region presents the lattice oxygen signature and several other peaks, including one at 533.5 eV characteristic of water molecules adsorbed on TiO_2 surface and other species such as NO_2 (536.8 eV).[8] In the absence of NO_2, no carbon contamination was observed (Figure 1d). The detection of a carbon signature is likely due to the displacement of carbonaceous residues from chamber walls by NO_2. Displacement of species adsorbed on chamber walls has been previously described for similar APXPS experiments.[9] On the basis of the relative intensities of C1s and N1s signals and their core level cross sections, we estimate the C/N ratio to be ~3. Whereas these species coexist on the TiO_2 surface, our results show no evidence of reactions between carbonaceous species and NO_x under UV irradiation, as illustrated by the lack of change in the C1s signatures (Figure S1 in the Supporting Information), by the rapid healing of TiO_2 defects upon introduction of NO_2 (Figure S2 in the Supporting Information), and by the absence of new signatures attributable to C−N moieties.

Under 0.05 Torr of NO_2, the contribution of gas-phase molecules to the intensity of the surface peaks cannot be entirely ruled out. Although the position of the $NO_{2,gas}$ peak in the surface N1s region could not be confirmed, it could slightly contribute to the intensity of the peak at 407.5 eV. Gas-phase NO_2 also appears in the surface O1s region at 536.8 eV (Figure 1c). Its intensity was used to estimate the potential contribution of $NO_{2,gas}$ to the surface N1s peak at 407.5 eV, which is accounted for in the error bars (Figure 2). More details of the

assignment of gas-phase N1s signals and their contribution to surface spectra can be found in the Supporting Information (Figures S3 and S4).

The adsorption of NO_2, NO, and N_2O has been extensively studied on TiO_2,[9−11] Fe_2O_3,[12] Al_2O_3,[12] and aluminum-,[13] magnesium-,[13] and nitrogen-containing minerals.[14] Reported adsorbed species at room temperature are NO_3^- (407.0 to 407.6 eV),[9,11,12,14] physisorbed NO_2 (405.4 to 406.0 eV),[11,14] $NO_{2,chem.}$ or NO_2^- (403.5 to 404.0 eV),[9,11,12,14] NO (400.5 to 403 eV),[10,12,13] and atomic N (396.8 to 400 eV).[9,11,12] The main product of NO_2 adsorption is the nitrate anion, formed through a disproportionation process:[15]

$$2NO_{2,ads} \rightarrow NO_{3,ads}^- + NO_{ads}^+ \tag{1}$$
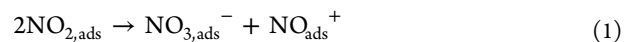
NO_2 adsorption in the dark yields four different types of surface-bound species at 407.5, 405.6, 403.1, and 400.8 eV (Figure 1a), which were therefore attributed to NO_3^- (407.5 eV), to weakly adsorbed NO_2 (405.6 eV), and tentatively to $NO_{2,chem.}/NO_2^-$ (noted NO_2^- in this article) (403.1 eV) and N_{red} (400.8 eV). The variety of nitrogenated species observed can be attributed to the initial presence of surface defects prior to NO_2 introduction. A small fraction of stable NO_2^- may be associated with the defect healing process observed when NO_2 was admitted in the chamber (Figure S2 in the Supporting Information). The peak at 400.8 eV is positioned between the usually reported binding energies for NO and N, and whereas all the peaks were fitted with narrow fwhm (1.3 to 1.7 eV), this contribution was larger (3 eV), indicating the possible presence
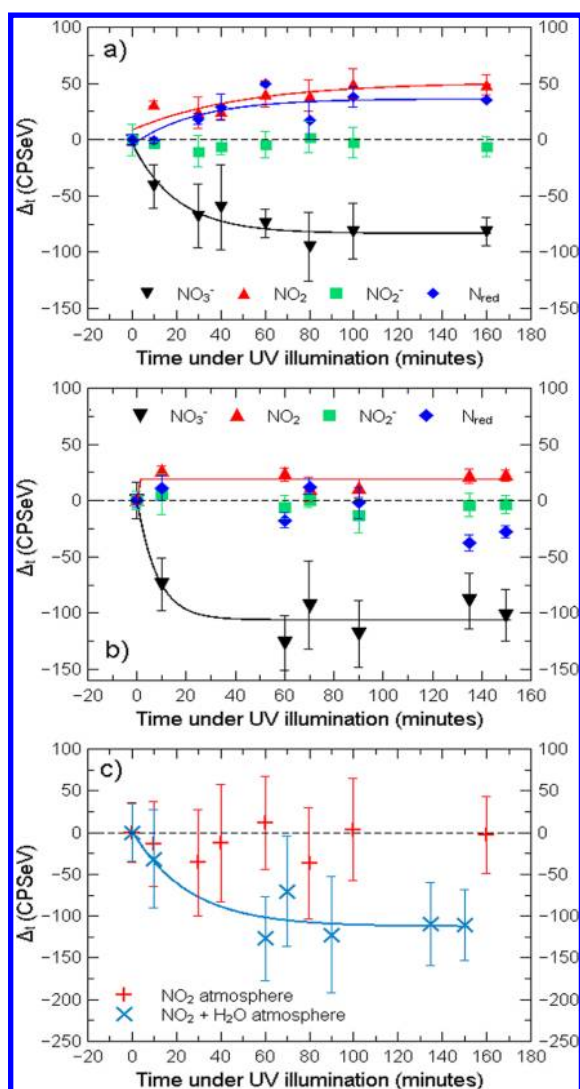
Figure 2. Time evolution of surface species for 0.05 Torr NO_2 under UV irradiation (a) without humidity and (b) with humidity (0.05 Torr H_2O). (c) Nitrogen mass balance on the surface of the anatase single crystal during UV irradiation, under 0.05 Torr of NO_2 without and with humidity.

of several reduced nitrogenated species, such as NO^+, NO^{-}, and N^+, as previously suggested,[12] or different adsorption modes of NO.[13] The weakly adsorbed NO_2 peak was fitted with two contributions to reflect its paramagnetic nature, with a binding energy difference of 0.7 eV and an intensity ratio of 3:1.[16,17] Evolution of these signals as a function of NO_2 pressure is shown in Figure S5 in the Supporting Information.
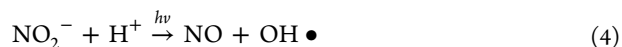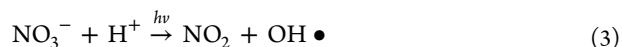
A UV LED (365 nm, 0.6 mW/cm²) was used to irradiate the sample while monitoring surface species by APXPS. The parameter $\Delta_t(i) = [N_i]_t - [N_i]_0$ was defined as the difference between the absolute area of the peak of the ith nitrogen species at irradiation time t, $[N_i]_t$, and the corresponding signal measured in the dark at the beginning of the experiment ($t = 0$), $[N_i]_0$. Error bars represent the standard deviation between two experimental values taken under the same conditions in two different areas of the sample and, for the peak at 407.5 eV, the potential contribution of $NO_{2,gas}$ to the evolution of its intensity.

Upon irradiation ($t > 0$ min) under 0.05 Torr of NO_2, the NO_3^- signal decreased, whereas those of NO_2 and N_{red}
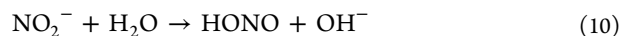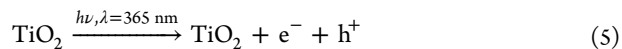
increased (Figure 2a). The same experiment was repeated under 0.05 Torr of NO_2 + 0.05 Torr of H_2O (Figure 2b) showing a similar trend for NO_3^-, with a sharp decrease in intensity within the first minutes of irradiation. However, NO_2 and N_{red} signals were constant. The overall nitrogen mass balance for the reactions occurring at the TiO_2 surface in absence of humidity was close to zero, but it was negative in the presence of humidity (Figure 2c), indicating a loss of nitrogenated species to the gas phase due to reactions of NO_3^- under UV irradiation in the presence of water.

A common thread connecting the evolution of the surface spectra under UV light in these two experiments with NO_2 or NO_2/H_2O mixtures is the photoinduced conversion of nitrate on anatase. These reactions were not induced by beam damage due to exposure of TiO_2 to the X-rays (see "Experimental methods" in the Supporting Information) and can be explained by photolytic and/or photocatalytic processes.

NO_3^- adsorbed on photoinactive surfaces can undergo photolysis under UV light according to reactions 2−4:[18,19]

$$NO_3^- \xrightarrow{h\nu} NO_2^- + O(^3P) \tag{2}$$

$$NO_3^- + H^+ \xrightarrow{h\nu} NO_2 + OH \bullet \tag{3}$$

$$NO_2^- + H^+ \xrightarrow{h\nu} NO + OH \bullet \tag{4}$$

In the presence of a photoactive material, other mechanisms need to be taken into consideration. Irradiation at 365 nm generates electron/hole (e^-/h^+) pairs in anatase (bandgap: 3.2 eV, eq 5). These species then migrate to the surface of the crystal, where they can react with adsorbed compounds, ultimately leading to the formation of reduced nitrogenated species (eqs 6−10, all species are adsorbed):[3,5]

$$TiO_2 \xrightarrow{h\nu, \lambda=365\ nm} TiO_2 + e^- + h^+ \tag{5}$$

$$NO_3^- + h^+ \rightarrow NO_3 \bullet \tag{6}$$

$$NO_2 + e^- \rightarrow NO_2^- \tag{7}$$

$$NO_3\bullet \xrightarrow{h\nu} NO + O_2 \tag{8}$$

$$NO_3\bullet \xrightarrow{h\nu} NO_2 + O \bullet \tag{9}$$

$$NO_2^- + H_2O \rightarrow HONO + OH^- \tag{10}$$

The photoadsorption cross-section of adsorbed NO_3^- for reaction 2 was reported to be 1.09×10^{-18} cm²/molecule at 305 nm and one order of magnitude lower (1.0×10^{-19} cm²/molecule) at 365 nm.[20] Although evidence of the photolysis of NO_3^- at 305 nm on photoinert surfaces exists, for example, on alumina[19] or silica,[21] Ndour et al.[3] have shown that steps 6 and 7 are essential for the generation of NO_x in the gas phase from adsorbed NO_3^- under UV irradiation at 365 nm such as the one used in this study. The results presented in Figure 2a are in good agreement with the mechanisms described by eqs 5 to 10. In the absence of water, adsorbed NO_3^- was mainly converted to adsorbed NO_2 and N_{red}, and the surface nitrogen mass balance was close to zero (Figure 2c). When water vapor was introduced in the chamber (0.05 Torr H_2O), the UV-induced conversion of NO_3^- generated gas phase products and the nitrogen mass-balance became negative. According to eqs 5 to 10, the most likely gas-phase products formed are NO and HONO. Bedjanian et al.[5] found a humidity threshold for

HONO production close to 0.1% RH for the interaction of NO_2 with TiO_2 under UV irradiation. This relative humidity corresponds to a partial pressure of ~0.02 Torr of H_2O at 293 K in our system. Gas-phase HONO formation is therefore expected under the conditions used here. Finally, although the intensity of the NO_2^- peak did not change significantly in any of these experiments, its contribution to the above-mentioned reactions cannot be ruled out if the lifetime of photogenerated NO_2^- is much shorter than the scanning time due to reactions 4 and 10.

Gas-Phase Spectra. The gas-phase composition was also monitored as a function of irradiation time to verify the hypothesis that the reaction of NO_3^- species adsorbed on TiO_2 produced gas-phase compounds under UV light. In these experiments, the sample was fully retracted so that the synchrotron X-rays could probe the gas phase to monitor the UV-induced changes in the oxidation state of the gaseous molecules (see Figure S8 in the Supporting Information for experimental setup). Figure 3a presents a gas-phase spectrum
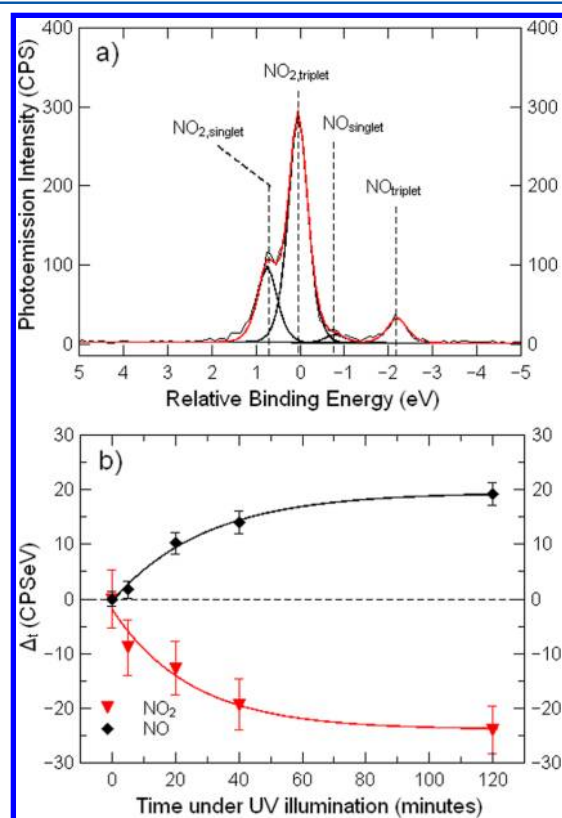

Figure 3. (a) N1s APXPS gas phase spectrum at 0.05 Torr of NO_2 in the dark at 293 K (red curve). The black curves show the deconvolution of the peaks into components of the NO_2 and NO species. (b) Time evolution of gas phase species during UV irradiation of the gas phase only. Error bars are estimated as 10% of the raw intensities measured for NO_2 and NO.

obtained in the dark. The energy scale in these spectra is the vacuum level of the analyzer entrance electrode. Figure 3a is plotted on a relative energy scale, with origin in the NO_2 triplet peak. Assuming that the main peak can be assigned to NO_2, the N1s gas phase signal was fitted with four peaks attributed to two paramagnetic species: NO_2 triplet (0 eV), NO_2 singlet (+0.7 eV), NO triplet (−2.17 eV), and NO singlet (−0.77 eV).[16] The triplet to singlet ratio was fixed using the statistical

value of 3:1 for the $^3\Pi$ and $^1\Pi$ ionic states.[17] The initial presence of NO is likely due to disproportionation of NO_2 on the stainless-steel walls of the chamber and gas lines (eq 1).[15]

The evolution of the gas-phase composition with time under UV irradiation was then investigated in a two-step process under 0.05 Torr of NO_2 in the absence of water and 0.05 Torr of NO_2 + 0.05 Torr of H_2O. First, the TiO_2 single crystal was fully retracted and only the gas phase was irradiated with UV light for 2 h to monitor the changes induced by gas-phase reactions. In a subsequent experiment, gas-phase spectra were taken prior to introducing the anatase sample in the path of the X-ray and UV beams (Figure S8 in the Supporting Information) and again after 2 h of UV irradiation of the TiO_2 to measure how surface reactions contributed to the gas-phase composition. Under UV irradiation, the final gas-phase composition was found to be identical in both cases.

The geometry of the UV irradiation caused the entire chamber to be exposed to low intensity UV, in addition to the highly intense UV beam focused on the sample position. A net production of NO was observed, associated with a simultaneous depletion of NO_2 (Figure 3b). It can be attributed to NO_2 photolysis in the gas phase (eq 11).[22] The observed reaction rate (2×10^{-4} to 2×10^{-5} s^{-1}) is in good agreement with that expected from the measured irradiance inside the chamber (5×10^{-4} to 10^{-5} s^{-1}) (Figure S9 in the Supporting Information).

$$NO_2(g) \xrightarrow{h\nu\,\lambda<420\,nm} NO(g) + O(^3P) \qquad (11)$$
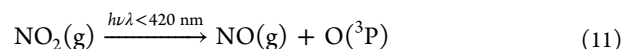
The same analysis presented in Figure S9 in the Supporting Information concluded that surface reactions of NO_2 adsorbed to the chamber walls did not contribute to the composition of the gas phase under UV irradiation.

When the experiment was repeated while irradiating the sample, the same final gas-phase composition was obtained, and the anatase single crystal was found to contribute neither to the NO generation nor to the production of any other gas phase species in detectable amounts. Assuming that the partial pressure needs to be at least 10^{-3} Torr for a gas-phase compound to be clearly discernible and given the volume of the chamber (1500 cm^3) and the surface area of the single crystal (25 mm^2, assuming no porosity), the turnover number for a surface reaction to generate a significant amount of gas phase product in 2 h would need to be at least three to four orders of magnitude higher than previously reported (64 to 848 $\times 10^{-9}$ mol m^{-2} s^{-1}).[23] Although the gas-phase spectra could not confirm the creation of new gas-phase products by surface reactions (NO, HONO, N_2O), their generation cannot be ruled out. HONO produced during irradiation may also decompose fast with UV at $\lambda = 365$ nm according to reaction 12, thus preventing its accumulation in the gas phase:[22]

$$HONO(g) \xrightarrow{h\nu\,\lambda<400\,nm} NO(g) + OH(g) \qquad (12)$$
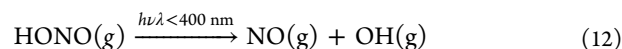
Efficient Trapping by Coadsorbed Cations. Potassium can be a contaminant in these experiments, diffusing from the heater or from the bulk of the single crystal to the surface. Berkó et al. have shown that 1 to 2 nm potassium clusters can be grown by annealing the TiO_2 single crystal ($T > 675$ K) and they are preferentially cation-terminated.[24] After several cycles of annealing in oxygen (10^{-5} Torr) at 773 K, clusters of potassium were grown on the surface of the anatase single crystal, as verified by taking spectra in the K2p region around 293 eV. The presence of K$^+$ matched a sharp increase in the NO_3^- peak intensity (Figure 4a and inset). Lowering the
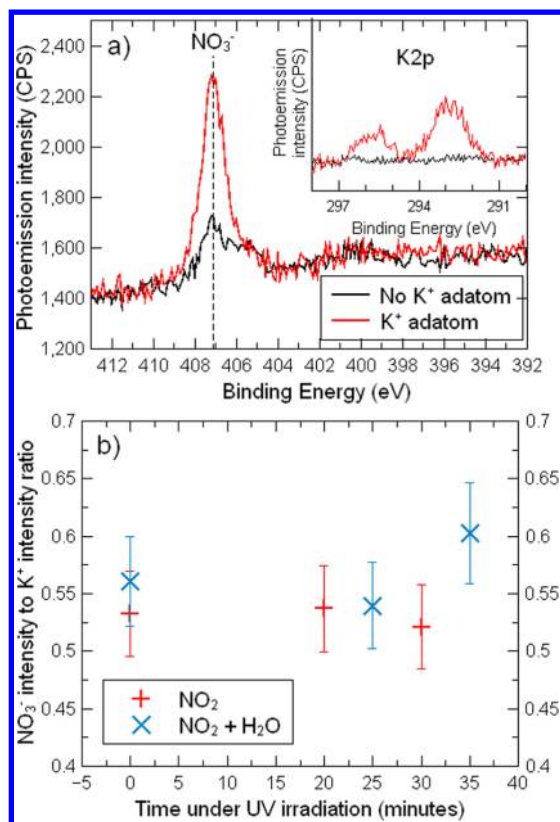
Figure 4. (a) N1s surface signals showing a strong increase in the NO_3^- peak (red line) correlated to the presence of potassium at the surface compared to a potassium-free area (black line) Inset: Corresponding K2p region showing the presence of potassium on the anatase single crystal. (b) Time evolution of the NO_3^-/K^+ ratio on the surface under UV irradiation in 0.05 Torr of NO_2 without and with addition of 0.05 Torr of H_2O. NO_3^- and K^+ intensities were normalized using the O1s baseline as a reference.

pressure in the chamber from 5×10^{-2} Torr to 5×10^{-7} Torr did not remove this NO_3^- feature, indicating a strong adsorption, in contrast with the behavior observed in the absence of K^+ (Figure S5 in the Supporting Information). Figure 4b shows the evolution of the ratio of NO_3^- to K^+ peak intensities under 0.05 Torr of NO_2 or under 0.05 Torr of NO_2 + 0.05 Torr of H_2O with time under UV irradiation.

Under both conditions, this ratio is constant throughout the experiment, indicating that the NO_3^- species coupled to K^+ are not reactive and stay on the surface, unlike what was previously observed for weakly adsorbed NO_3^- (Figure 2a,b). Nitrate ions adsorbed in the vicinity of potassium are effectively trapped and do not react. The deposition of K^+ on TiO_2 results in a localized reduction of the substrate by electron transfer: the negative charge is delocalized to the adjacent Ti ions, leaving the K^+ cluster positively charged.[25] Ion pairing ($K^+NO_3^-$) and electronic repulsion between the cationic potassium cluster and the photogenerated holes (h^+) can explain the absence of conversion of NO_3^- species coupled to K^+ as reaction 6 is hindered.

In summary, several surface species were found when TiO_2 was exposed to NO_2. Their reaction under UV light led to the formation of reduced nitrogenated species. In the absence of humidity, NO_3^- was predominantly converted to adsorbed NO_2 and potentially NO^+, NO^-, and N^+, identified as N_{red}. Traces of humidity in the chamber (0.05 Torr of H_2O, i.e., 0.3%

RH) drove the conversion of NO_3^- toward the formation of gas phase products, which could not be detected in the gas phase by APXPS due either to their low concentration or their reactivity under UV. The presence of cationic adatoms (K^+) enhanced the adsorption of NO_3^- and hindered its photocatalytic conversion, thus inhibiting the formation of by-products. These results contribute to understanding the role of TiO_2 as either a source or a sink of atmospheric nitrogenated compounds. The reactivity of NO_x and NO_3^- on surfaces leading to reduced adsorbed and gas-phase nitrogenated species needs to be considered in the engineering of depolluting materials and incorporated in atmospheric models. Differences can be expected at lower NO_x concentrations (ppb range), arising from several factors such as the presence of lower NO_2/water and NO_2/O_2 ratios. It should also be considered that NO_x is rarely in contact with pristine metal oxide surfaces. Atmospheric particles and urban surfaces are coated with complex organic soiling layers composed primarily of carbonaceous constituents, which are likely to be involved in surface reactions.[26,27] Self-cleaning, depollution (*DeNOx*) and *renoxification* processes are likely to be affected by the presence of heteroatoms present as impurities, dopants, and atmospheric soiling on the TiO_2 surface.

■ EXPERIMENTAL METHODS

The measurements were carried out at beamline 11.0.2 of the Advanced Light Source at Lawrence Berkeley National Laboratory. This instrument is designed for in situ measurements of chemical reactions at pressures of up to 5 Torr, which allowed probing the surface of the catalyst under realistic regimes with synchrotron radiation. All experiments involving TiO_2 were conducted using an anatase (101) single crystal purchased from Surface Preparation Lab (Netherlands). Sample illumination was performed with a UV-LED with a narrow emission band centered around 365 nm. More details about sample preparation, APXPS setup, UV irradiation, and peak fitting are given in the Supporting Information.

■ ASSOCIATED CONTENT

ⓈSupporting Information
Peak fitting methodology, experimental details. This material is available free of charge via the Internet at http://pubs.acs.org.

■ AUTHOR INFORMATION

Corresponding Author
*E-mail: hdestaillats@lbl.gov.

Notes
The authors declare no competing financial interest.

■ REFERENCES

(1) Chen, J.; Poon, C. Photocatalytic Construction and Building Materials: From Fundamentals to Applications. *Build. Environ.* **2009**, *44*, 1899−1906.

(2) Dalton, J. .; Janes, P. .; Jones, N. .; Nicholson, J. .; Hallam, K. .; Allen, G. Photocatalytic Oxidation of NO_x Gases Using TiO_2: A Surface Spectroscopic Approach. *Environ. Pollut.* **2002**, *120*, 415−422.

(3) Ndour, M.; Conchon, P.; D'Anna, B.; Ka, O.; George, C. Photochemistry of Mineral Dust Surface as a Potential Atmospheric Renoxification Process. *Geophys. Res. Lett.* **2009**, *36*, L05816.

(4) Monge, M. E.; George, C.; D'Anna, B.; Doussin, J.-F.; Jammoul, A.; Wang, J.; Eyglunent, G.; Solignac, G.; Daele, V.; Mellouki, A. Ozone Formation from Illuminated Titanium Dioxide Surfaces. *J. Am. Chem. Soc.* **2010**, *132*, 8234−8235.

(5) Bedjanian, Y.; El Zein, A. Interaction of NO_2 with TiO_2 Surface Under UV Irradiation: Products Study. *J. Phys. Chem. A* **2012**, *116*, 1758−1764.

(6) Gustafsson, R. J.; Orlov, A.; Griffiths, P. T.; Cox, R. A.; Lambert, R. M. Reduction of NO_2 to Nitrous Acid on Illuminated Titanium Dioxide Aerosol Surfaces: Implications for Photocatalysis and Atmospheric Chemistry. *Chem. Commun.* **2006**, 3936−3938.

(7) Ogletree, F. D.; Bluhm, H.; Hebenstreit, E. D.; Salmeron, M. Photoelectron Spectroscopy Under Ambient Pressure and Temperature Conditions. *Nucl. Instrum. Methods Phys. Res., Sect. A* **2009**, *601*, 151−160.

(8) Ketteler, G.; Yamamoto, S.; Bluhm, H.; Andersson, K.; Starr, D. E.; Ogletree, D. F.; Ogasawara, H.; Nilsson, A.; Salmeron, M. The Nature of Water Nucleation Sites on TiO_2(110) Surfaces Revealed by Ambient Pressure X-Ray Photoelectron Spectroscopy. *J. Phys. Chem. C* **2007**, *111*, 8278−8282.

(9) Haubrich, J.; Quiller, R. G.; Benz, L.; Liu, Z.; Friend, C. M. In Situ Ambient Pressure Studies of the Chemistry of NO_2 and Water on Rutile TiO_2(110). *Langmuir* **2010**, *26*, 2445−2451.

(10) Herranz, T.; Deng, X.; Cabot, A.; Liu, Z.; Salmeron, M. In Situ XPS Study of the Adsorption and Reactions of NO and O_2 on Gold Nanoparticles Deposited on TiO_2 and SiO_2. *J. Catal.* **2011**, *283*, 119−123.

(11) Rodriguez, J. A.; Jirsak, T.; Liu, G.; Hrbek, J.; Dvorak, J.; Maiti, A. Chemistry of NO_2 on Oxide Surfaces: Formation of NO_3 on TiO_2(110) and NO_2↔O Vacancy Interactions. *J. Am. Chem. Soc.* **2001**, *123*, 9597−9605.

(12) Baltrusaitis, J.; Jayaweera, P. M.; Grassian, V. H. XPS Study of Nitrogen Dioxide Adsorption on Metal Oxide Particle Surfaces Under Different Environmental Conditions. *Phys. Chem. Chem. Phys.* **2009**, *11*, 8295−8305.

(13) Au, C. T.; Carley, A. F.; Roberts, M. W. Photoelectron Spectroscopy: A Strategy for the Study of Reactions at Solid Surfaces. *Int. Rev. Phys. Chem.* **1986**, *5*, 57−87.

(14) Aduru, S.; Contarini, S.; Rabalais, J. W. Electron-, X-Ray-, and Ion-Stimulated Decomposition of Nitrate Salts. *J. Phys. Chem.* **1986**, *90*, 1683−1688.

(15) Finlayson-Pitts, B. J.; Wingen, L. M.; Sumner, A. L.; Syomin, D.; Ramazan, K. A. The Heterogeneous Hydrolysis of NO_2 in Laboratory Systems and in Outdoor and Indoor Atmospheres: An Integrated Mechanism. *Phys. Chem. Chem. Phys.* **2003**, *5*, 223−242.

(16) Siegbahn, K.; Nordling, C.; Johansson, G.; Hedman, J.; Heden, P.; Hamrin, K.; Gelius, U.; Bergmark, T.; Werme, L.; Manne, R. et al. *ESCA Applied to Free Molecules*; North Holland Publishing Company: Amsterdam, 1969.

(17) Hosaka, K.; Adachi, J.; Takahashi, M.; Yagishita, A. N 1s Photoionization Cross Sections of Nitric Oxide Molecules in the Shape Resonance Region. *J. Phys. B: At., Mol. Opt. Phys.* **2003**, *36*, 4617−4629.

(18) Mack, J.; Bolton, J. R. Photochemistry of Nitrite and Nitrate in Aqueous Solution: A Review. *J. Photochem. Photobiol., A* **1999**, *128*, 1−13.

(19) Rubasinghege, G.; Grassian, V. H. Photochemistry of Adsorbed Nitrate on Aluminum Oxide Particle Surfaces. *J. Phys. Chem. A* **2009**, *113*, 7818−7825.

(20) Du, J.; Zhu, L. Quantification of the Absorption Cross Sections of Surface-Adsorbed Nitric Acid in the 335−365 nm Region by Brewster Angle Cavity Ring-down Spectroscopy. *Chem. Phys. Lett.* **2011**, *511*, 213−218.

(21) Goodman, A. L.; Underwood, G. M.; Grassian, V. H. Heterogeneous Reaction of NO_2: Characterization of Gas-Phase and Adsorbed Products from the Reaction, $2NO_2(g) + H_2O(a) \rightarrow HONO(g) + HNO_3(a)$ on Hydrated Silica Particles. *J. Phys. Chem. A* **1999**, *103*, 7217−7223.

(22) Finlayson-Pitts, B. J.; Pitts, J. N. *Chemistry of the Upper and Lower Atmosphere*; Academic Press: San Diego, CA, 2000.

(23) Dillert, R.; Stötzner, J.; Engel, A.; Bahnemann, D. W. Influence of Inlet Concentration and Light Intensity on the Photocatalytic Oxidation of Nitrogen(ii) Oxide at the Surface of Aeroxide® TiO_2 P25. *J. Hazard. Mater.* **2012**, *211−212*, 240−246.

(24) Berkó, A.; Balázs, N.; Kassab, G.; Óvári, L. Segregation of K and Its Effects on the Growth, Decoration, and Adsorption Properties of Rh Nanoparticles on TiO_2(110). *J. Catal.* **2012**, *289*, 179−189.

(25) Bredow, T.; Aprà, E.; Catti, M.; Pacchioni, G. Cluster and Periodic Ab-Initio Calculations on K/TiO_2(110). *Surf. Sci.* **1998**, *418*, 150−165.

(26) Sleiman, M.; Ban-Weiss, G.; Gilbert, H. E.; François, D.; Berdahl, P.; Kirchstetter, T. W.; Destaillats, H.; Levinson, R. Soiling of Building Envelope Surfaces and Its Effect on Solar Reflectance—Part I: Analysis of Roofing Product Databases. *Sol. Energy Mater. Sol. Cells* **2011**, *95*, 3385−3399.

(27) Poulston, S.; Twigg, M. V.; Walker, A. P. The Effect of Nitric Oxide on the Photocatalytic Oxidation of Small Hydrocarbons Over Titania. *Appl. Catal., B* **2009**, *89*, 335−341.